ATTENUATION RELATIONS OF STRONG MOTION IN JAPAN USING SITE CLASSIFICATION BASED ON PREDOMINANT PERIOD

Toshimasa Takahashi, Akihiro Asano, Hidenobu Okada
Shikoku Electric Power Co. Inc., Takamatsu, Japan
Taketoshi Saiki
Yonden Consultants Co.,Inc., Kagawa, Japan
Kojiro Irikura
DPRI, Kyoto University, Kyoto, Japan
John X. Zhao, Jian Zhang
Institute of Geological & Nuclear Sciences, Lower Hutt, New Zealand
Hong K. Thio, Paul G. Somerville
URS Corporation, Pasadena, CA 91101-2560, USA
Yasuhiro Fukushima
Japan Engineering Consultants CO.,LTD., Tokyo, Japan
Yoshimitsu Fukushima
Ohsaki Research Institute Co., Inc., Japan

Abstract

A spectral acceleration attenuation model for Japan is presented. The data set includes a very large number of strong ground motion records up to the end of 2003. Site class terms, instead of individual site correction terms, are used based on a recent study on site classification for strong motion recording stations in Japan. By using site class terms, tectonic source type effects are identified and accounted in the present model. Effects of faulting mechanism for crustal earthquakes are also accounted for. For crustal and interface earthquakes, a simple form of attenuation model is able to capture the main strong motion characteristics and achieves unbiased estimates. For subduction slab events, a simple distance modification factor is employed to achieve plausible and unbiased prediction. Effects of source depth, tectonic source type, and faulting mechanism for crustal earthquakes are significant.

Introduction

Many attenuation relations for strong ground motion have been developed as an important component of seismic hazard studies. In a deterministic manner engineers also use attenuation models to estimate the forces and/or displacements induced in engineering structures. In a probabilistic seismic hazard analysis, both the mean values and the prediction uncertainties of an attenuation model are utilized, and high model prediction uncertainties can lead to high probabilistic ground motion estimates.

Japan is located at a plate boundary and, therefore, has a complicated geological and tectonic setting. Because the paths from fault ruptures of its earthquakes to the ground surface vary from one type of earthquake to another, the ground motions generated by different types of earthquakes are expected to be different even if the events have identical magnitudes and source distances. In the past, spectral attenuation models developed for earthquakes in Japan have not usually accounted for tectonic source type, though different attenuation characteristics between interface and slab events were widely recognized.

The site conditions at a recording station have a very strong influence on ground motions induced by earthquakes, and a significant amount of effort on collecting geotechnical information for recording stations has been made in both Japan and elsewhere. Up until now, the majority of the strong motion stations in Japan have had limited geotechnical information. Researchers in Japan have attempted to overcome this difficulty by assigning individual site terms for each recording station (e.g.: Molas & Yamazaki 1995, Kobayashi *et al*. 2000, and Takahashi *et al*. 2004). A possible drawback to this approach is that model's prediction error and some of the source effects may propagate into individual site terms. With the reasonably reliable site classifications assigned by Zhao *et al.* (2004), however, we are able to evaluate the effects of tectonic source type and faulting mechanism for crustal earthquakes.

Strong-motion data set

The magnitude and source distance (defined in Equations 1 and 2 in the next section) distribution for earthquakes with focal depths of up to 162 km is shown in Figure 1(a) for the Japanese strong-motion data set, and Figure 1(b) for the overseas data sets used in the modelling. In order to eliminate the bias that could be introduced by untriggered instruments, data for the modelling were selected from a much larger data set by exclusion of data at distances larger than a specified value for a given magnitude (see Figure 1(a)). For subduction slab events, the maximum source distance was set to 300km. There are only a small number of records within 30km source distance in the Japanese data set, and all near source data within 10km are from the 1995 Kobe earthquake and the 2000 Tottori earthquake. The overseas data from the western part of the USA and the 1978 Tabas Iran earthquake provide a small but valuable amount of additional data within 40km source distance and these records were used primarily to constrain the near-source behaviour of the model. Magnitude and focal depth distributions for the Japanese data are shown in Figure 1(c) for crustal and subduction earthquakes. There is a reasonably good distribution of data for all magnitude and focal depth ranges, and the records from deep slab events provide good constraint to the depth term of the attenuation model. The maximum depth for crustal earthquakes was set to 25km, and 50km for interface events. Figure 1(d) shows a strong correlation between focal depth and source distance, because focal depth contributes to the distance, especially for slab events. We found that the epicentral latitudes and longitudes and focal depths determined by JMA were not consistent with those determined by other seismological organizations, and so the relocated ISC locations and depths were used in the present study. The moment magnitudes are from the Harvard catalogue unless moment magnitude from a special study is available.

Table 1 shows the break down of record numbers by source type and focal mechanism categories. Among the total of 4518 Japanese records, 1285 are from crustal events, 1508 are from interface events and 1725 are from slab events. For crustal events, many published attenuation models show that events with reverse-faulting mechanisms produce higher ground motions than strike-slip events. The number of records from reverse-fault events is large enough for the present study to account for the possible difference between the ground motions from reverse and strike-slip events (see Table 1). The very small number of records from crustal events with normal faulting mechanisms does not warrant the normal-fault events being considered as a separate group.

The data from the western part of the USA are all from crustal earthquakes (except for a 1992-04-25 event that was identified as an interface event) with focal depths less than 20km. Of the total of 196 near-source records from crustal earthquakes, 123 records are from reverse-faulting events and 73 records are from strike-slip events. For the overseas interface event, 12 near-source records were used.

Table 1Numbers of records by source type, faulting mechanism, and region

Japan				
Focal mechanism	Crustal	Interface	Slab	Total for each focal mech.
Reverse	250	1492	408	2150
Strike-slip	1011	13	574	1598
Normal	24	3	735	762
Unknown			8	8
Total for each source type	1285	1508	1725	4518
Iran and Western USA				
Reverse	123	12		135
Strike-slip	73			73
Total for each source type	196	12		208
Total for each source type from all regions				Grand total
	1481	1520	1725	4726

Model development

In the present study, the random-effects model of Abrahamson and Youngs (1992) was used. When there is a strong correlation between magnitude and source distance, an ordinary least-squares approach will not give a set of true estimates of the model's coefficients. At the present study, the following simple form of the attenuation function was selected:

$$\log_e[y_{i,j}(T)] = aM_w + bx_{i,j} - \log_e(r_{i,j}) + e(h - h_c)\delta_h + S_R + S_I + S_S + S_{SL}\log_e(x) + S_k + \xi_{i,j} + \eta_i \qquad (1)$$

$$r_{i,j} = x_{i,j} + \mathrm{c}\exp(dM_i) \qquad (2)$$

where y is either peak ground acceleration (PGA) in cm/s^2 or 5% damped acceleration response spectrum (the geometric mean of two horizontal components) in cm/s^2 for a spectral period T, M_w is moment magnitude, x is source distance in km, and h is focal depth in km. The reverse-fault parameter S_R applies only to crustal events with a reverse-faulting mechanism and is zero for all other events. The tectonic source-type parameter S_I applies to interface events and is 0 for all other type events, and S_S applies to subduction slab events only and is zero for all other type events. S_{SL} is a magnitude-independent path modification term for slab events to compensate for the complex seismic wave travel-path for slab events. S_k is the site-class term for a given site class, with the four site classes used in the present study, SC I, II, III and IV, approximately corresponding to the four classes, rock, hard soil, medium soil and soft soil, as defined in Molas & Yamazaki (1995). See also Table 2 that shows the approximately corresponding site classes defined by the Building Seismic Safety Council (2000). Subscript i denotes event number and j denotes record number from event i. Coefficient "h_c" is a depth constant. When h is larger than h_c, the depth term e(h-h_c) takes effect, with δ_h being a dummy variable that equals 0 for $h < h_c$ and 1 for $h \geq h_c$. When h is larger than 125km, h=125km is selected so that a constant factor is used for deeper earthquakes. Random variable $\xi_{i,j}$ is associated with intra-event errors (errors that represent uncertainties between recording stations in a given event) with zero mean and a standard deviation of σ, and random variable η_i is associated with inter-event errors (errors that represent uncertainties between earthquakes) with zero mean and a standard deviation of τ. Coefficients "a", "b", "c", "d" and "e", site class term S_k, reverse-fault term S_R and source-type terms

S_I, S_S and S_{SL} are determined by regression analysis for each period. Source distance x is the shortest distance to the rupture zone for earthquakes with available fault models, and hypocentral distance for the other events.

Table 2 Site class definitions used in the present study and the approximately corresponding NEHRP site classes (BSSC 2000)

Site class	Description	Natural period	V_{30} calculated from site period	NEHRP site classes
SC I	Rock	T < 0.2s	$V_{30} > 600$	A+B
SC II	Hard soil	0.2 = T < 0.4s	$300 < V_{30} = 600$	C
SC III	Medium soil	0.4 = T < 0.6s	$200 < V_{30} = 300$	D
SC IV	Soft soil	T = 0.6s	$V_{30} = 200$	E+F

The coefficients of the simple model in Equation (1) were derived from the data set and extensive residuals analysis was then carried out. The results of our analyses suggested that the simple model in Equation (1) predicts spectral accelerations that are reasonably unbiased for crustal and interface events, and not seriously biased for slab events, even when the coefficients of the magnitude, geometric spreading and anelastic attenuation terms are the same for all three types of events. The modification factor for slab events applies only to a source distance about 40km or larger, but this should pose no restrictions to most practical applications.

The total standard error of the model's prediction is defined by

$$\sigma_T = \sqrt{\sigma^2 + \tau^2} \qquad (3)$$

with σ and τ as defined above. Both intra- and inter-event errors σ and τ are period dependent, but are assumed independent of magnitude.

We used the value of 15km for the depth coefficient "h_c" in the present study, and positive and statistically significant estimates for the depth coefficient "e" were achieved for all periods. The coefficients of all the terms in Equations 1 and 2 are shown in Table 3. They differ considerably from those of the Takahashi *et al.* (2004) model. However the predicted spectra for much of the magnitude and distance range of the present model are similar to those predicted by the Takahashi *et al.* (2004) model. The differences possibly result from the inclusion of over 300 records from the Mw=8.3, 26 September 2003, interface event.

In some of the following comparisons with the models from other studies, a "mean model" is used to overcome the differences in site classification schemes. The mean model refers to that for which the S_R, S_I, S_S and S_{SL} terms in Equation (1) are all zero (i.e., strike-slip or normal crustal earthquakes) and the site term takes the mean value for the model S_M, as calculated in Equation (4),

$$S_M = \frac{S_I N_I + S_{II} N_{II} + S_{III} N_{III} + S_{IV} N_{IV} + S_{ID} N_{ID}}{N_I + N_{II} + N_{III} + N_{IV} + N_{ID}} \qquad (4)$$

where S is the mean value, and N is the number of records in a site class. Subscripts I, II, III, IV and ID denotes site classes I, II, II, IV and individual site terms (for those sites with 3 or more records but without site classes), and subscript M denotes the mean model (mean site conditions).

Twelve SC I stations, which yielded 1145 records, have average shear-wave velocities in the range 1020-2200m/s. They are referred to as hard rock sites in the present study. The average intra-event residuals were found to decrease with increasing shear-wave velocity for all periods. Assuming that the average shear-wave velocity of SC I sites is 700m/s, a function having a linear term $\log_e(V_s/700)$ (V_s in m/s), and a fourth order of polynomial of $\log_e(T)$ term, were fitted to the intra-event residuals from the hard rock sites so that the site term for hard rock sites could be calculated by adding the predicted intra-event residuals for a given period and shear-wave velocity to the corresponding site terms for SC I sites. As an example, the hard rock site terms S_H are presented in Table 3(b) for hard rock sites with V_S=2000m/s, together with all other coefficients.

Table 3(a) Coefficients for source and path terms of the model in the present study

Period	a	b	c	d	e	S_R	S_I	S_S	S_{SL}
PGA	1.101	-0.00564	0.0055	1.080	0.01412	0.251	0.000	2.607	-0.528
0.05	1.076	-0.00671	0.0075	1.060	0.01463	0.251	0.000	2.764	-0.551
0.10	1.118	-0.00787	0.0090	1.083	0.01423	0.240	0.000	2.156	-0.420
0.15	1.134	-0.00722	0.0100	1.053	0.01509	0.251	0.000	2.161	-0.431
0.20	1.147	-0.00659	0.0120	1.014	0.01462	0.260	0.000	1.901	-0.372
0.25	1.149	-0.00590	0.0140	0.966	0.01459	0.269	0.000	1.814	-0.360
0.30	1.163	-0.00520	0.0150	0.934	0.01458	0.259	0.000	2.181	-0.450
0.40	1.200	-0.00422	0.0100	0.959	0.01257	0.248	-0.041	2.432	-0.506
0.50	1.250	-0.00338	0.0060	1.008	0.01114	0.247	-0.053	2.629	-0.554
0.60	1.293	-0.00282	0.0030	1.088	0.01019	0.233	-0.103	2.702	-0.575
0.70	1.336	-0.00258	0.0025	1.084	0.00979	0.220	-0.146	2.654	-0.572
0.80	1.386	-0.00242	0.0022	1.088	0.00944	0.232	-0.164	2.480	-0.540
0.90	1.433	-0.00232	0.0020	1.109	0.00972	0.220	-0.206	2.332	-0.522
1.00	1.479	-0.00220	0.0020	1.115	0.01005	0.211	-0.239	2.233	-0.509
1.25	1.551	-0.00207	0.0020	1.083	0.01003	0.251	-0.256	2.029	-0.469
1.50	1.621	-0.00224	0.0020	1.091	0.00928	0.248	-0.306	1.589	-0.379
2.00	1.694	-0.00201	0.0025	1.055	0.00833	0.263	-0.321	0.966	-0.248
2.50	1.748	-0.00187	0.0028	1.052	0.00776	0.262	-0.337	0.789	-0.221
3.00	1.759	-0.00147	0.0032	1.025	0.00644	0.307	-0.331	1.037	-0.263
4.00	1.826	-0.00195	0.0040	1.044	0.00590	0.353	-0.390	0.561	-0.169
5.00	1.825	-0.00237	0.0050	1.065	0.00510	0.248	-0.498	0.225	-0.120

The PGAs predicted by the crustal and interface models are compared with data from crustal and interface earthquakes of magnitude 6.0 or larger in Figure 2(a). The PGA data have been normalized to magnitude 7.0, a focal depth of 20 km, crustal events with strike-slip mechanism and SC II site conditions. The model fits this subset of the data reasonably well. In particular the near-source data from SC I and II sites, in the source distance range of 0-10km, including data recorded in the Kobe 1995 earthquake. A few records of earthquakes in the western part of USA, are reasonably well predicted. The near-source records that were under-predicted are from SC III and IV sites where nonlinear response was considered to be substantial (Fukushima *et al.*, 2000). The predicted PGAs of slab models are compared with the normalized PGAs from subduction slab events in Figure 2(b).

Figures 3a and 3b show a comparison with PGAs predicted by the models of Fukushima *et al.* (2000) and Si & Midorikawa (1999). At all magnitudes, the crustal and interface models derived in the present study predicts reasonably similar PGAs to those predicted by the Fukushima *et al.* (2000) over reasonably large magnitude and distance ranges (Figure 3a) the mean site conditions. The Si &

Midorikawa (1999) models for crustal and interface earthquakes predict generally larger PGAs than those by the present model. At source (< 0.2km), the present model predicts a PGA of about 0.8g, while the Fukushima *et al*. (2000) model predicts a PGA of about 0.65g while the Si & Midorikawa (1999) model predicts a PGA of 0.92g, for M_w=7.0. Note that for a magnitude 5 earthquake with a focal depth of 20 km, a source distance less than 10 km may be impossible, because of the small rupture area for a magnitude 5 event.

Table 3(b) Coefficients for site class terms and prediction error

Period (s)	S_H	S_1	S_2	S_3	S_4	σ	τ	σ_T
PGA	0.293	1.111	1.344	1.355	1.420	0.604	0.398	0.723
0.05	0.939	1.684	1.793	1.747	1.814	0.640	0.444	0.779
0.10	1.499	2.061	2.135	2.031	2.082	0.694	0.490	0.849
0.15	1.462	1.916	2.168	2.052	2.113	0.702	0.460	0.839
0.20	1.280	1.669	2.085	2.001	2.030	0.692	0.423	0.811
0.25	1.121	1.468	1.942	1.941	1.937	0.682	0.391	0.786
0.30	0.852	1.172	1.683	1.808	1.770	0.670	0.379	0.770
0.40	0.365	0.655	1.127	1.482	1.397	0.659	0.390	0.766
0.50	-0.207	0.071	0.515	0.934	0.955	0.653	0.389	0.760
0.60	-0.705	-0.429	-0.003	0.394	0.559	0.653	0.401	0.766
0.70	-1.144	-0.866	-0.449	-0.111	0.188	0.652	0.408	0.769
0.80	-1.609	-1.325	-0.928	-0.620	-0.246	0.647	0.418	0.770
0.90	-2.023	-1.732	-1.349	-1.066	-0.643	0.653	0.411	0.771
1.00	-2.451	-2.152	-1.776	-1.523	-1.084	0.657	0.410	0.775
1.25	-3.243	-2.923	-2.542	-2.327	-1.936	0.660	0.402	0.773
1.50	-3.888	-3.548	-3.169	-2.979	-2.661	0.664	0.408	0.779
2.00	-4.783	-4.410	-4.039	-3.871	-3.640	0.669	0.414	0.787
2.50	-5.444	-5.049	-4.698	-4.496	-4.341	0.671	0.411	0.786
3.00	-5.839	-5.431	-5.089	-4.893	-4.758	0.667	0.396	0.776
4.00	-6.598	-6.181	-5.882	-5.698	-5.588	0.647	0.382	0.751
5.00	-6.752	-6.347	-6.051	-5.873	-5.798	0.643	0.377	0.745

The present study and the Si & Midorikawa (1999) study found that crustal and interface events on average produce similar PGAs. However, in the Si & Midorikawa (1999) model the PGAs from slab events are much larger than those from crustal and interface events, by a factor of 1.66 (Figure 3) while the model of the present study has a factor 1.56 for slab events at a source distance of 60km. Their model generally predicts considerably larger PGAs than the present model. The difference is likely to come from two sources. The number of events in their study was only a fraction of the number in the present study and the majority of their 127 slab event records were from two large intra-plate events (1993-01-15 Off Kushiro M_w=7.6 (51 records) and 1994-10-04 East Off Hokkaido M_w=8.3 event (41 records)). In the present dataset, 19 records are from the 1993-01-15 event, and 10 records from 1994-10-04 event due to distance truncation. Our residuals analysis shows that the inter-event errors for the 1994-10-04 event and 28-1-2000 event in the same area are large and the large ground motions from these events may be a local anomaly or a particular source effect of the large slab event (see the discussion on the M_w square term in the next section). The inter-event error for the 1993-01-15 event is very small, suggesting the present model predicts the records from this event very well.

Figure 4 shows the effects of focal mechanism, tectonic source types and focal depth. In the present study, the base model is for crustal earthquakes with strike-slip or normal focal mechanism at a focal depth of 15km or less. For slab events, the modification factor is distance dependent and the scale factors for distances of 40, 60, 80 and 150km are presented. Figure 4(a) shows that crustal events with reverse focal mechanism produce about 20-40% larger ground motions than that predicted by the base model. For PGA at 0.05s and 0.1s periods, the scale factors for interface events were set at 1.0 as the coefficients derived in the regression analysis were not statistically significant. Up to 0.4s, the scale factors for interface events are very small. Beyond 0.4s, ground motions produced by interface events decrease quickly with increasing period and at 5.0s ground motions from interface events are about 60% of the motions predicted by the base model (Figure 4(a)). At a source distance of 40km, the scale factors for slab events are over 1.6 up to 0.7s, then decrease to about 1.0 at 2.0s period, while the scale factors at 150km have similar values to those for interface events. Figure 4(b) shows the effect of focal depth for the ground motions predicted by the present model. The scale factors decrease with increasing periods beyond 0.3s and the effect of focal depth is very large. However, there are very few data beyond 120km depth (the deepest event has a focal depth of 160km).

For an attenuation model used for a probabilistic seismic hazard study, uncertainty associated with the model has a very large effect on the level of the probabilistic ground motion. In Figure 5, comparison is made between the total prediction errors and those published previously. For crustal events shown in Figure 5(a), at periods less than 2.0s the total errors of the present study lie between the total errors from the Abrahamson & Silva (1997) model for M_W = 5 and 6 events. However at periods beyond 2.5s, the prediction errors of the present model are markedly smaller than those for M_W = 5 and 6 events and are similar to those for $M_W \geq 7$ events of the Abrahamson & Silva (1997) model. Figure 5(b) shows the total errors from the Youngs *et al.* (1997) model calculated for M_W =5, 6, 7, and 8 events, and those from the present model. The total errors of the present model for subduction events are significantly smaller than those from the Youngs *et al.* (1997) model for Mw=5 and 6 events (except at 0.1s period), especially for the interface events. Up to 1.5s, the total errors for interface events from the present study lie between those of the Youngs *et al.* (1997) model for Mw=7 and 8 events, and beyond 2s period the prediction errors for both interface and slab events are markedly smaller than those for Mw=8 events.

Figure 6(a) shows the variation of the amplification factors, with respect to the SC I sites, for the three soil classes. The amplification factors for a particular site class are the exponential of the difference between the site class terms and SC I site class terms, for example, $\exp(S_{III}-S_I)$ for SC III site class. The amplification curves are consistent with the definition of site class in terms of site dominant periods shown in Table 2. All three site classes show a trough at about 0.1s which can be interpreted as the period of the spectral peak for SC I sites. The amplification curve for SC II sites shows a broad-band amplification at periods beyond 0.15s. SC III class shows a peak amplification at about 0.5s which lies in the middle of dominant periods, 0.4-0.6s, for this site class. The amplification curve for SC IV sites has a peak at 0.9s that is also reasonably consistent with the definition of this site class having dominant periods larger than 0.6s. The corresponding spectral shapes, i.e., the spectral acceleration SA(T) (calculated from the model coefficients in Table 3) divided by PGA, for an M_W=7.0 event at a depth of 20km and a distance of 30km are shown in Figure 6(b) for crustal strike-slip and normal-fault events and four site classes. The peak values of the spectral shapes are between 2.0-2.5 and the spectral periods of the peaks increase with increasing site class which is consistent with the site classification scheme used in the present study.

Figure 7 shows the pseudo-velocity spectra for crustal, interface and slab events for M_W=7 events at 40 and 60km source distances. The strength of the spectra from slab events is evident, as is the reduction in elevation of the slab event spectra with increasing source distance.

Discussion and conclusions

An attenuation model accounting for tectonic source types and focal mechanisms of crustal events is derived in this study. The model predictions for all site classes and source types are plausible. The present model for crustal events predicts similar PGAs to those predicted by the Fukushima *et al*. (2000) model. Because of much smaller prediction error of the present model, we believe that the present model is more robust than the other models for subduction events.

The coefficients of the present model differ moderately from those of the Takahasi *et al.* (2004) model but the predicted spectra of crustal and interface events of the two models are very similar at nearly all periods. The response spectra predicted by the two models for slab events are also similar for source distances over 100km. At shorter distances, however, the present model predicts significantly higher short period spectra than the Takahasi *et al.* (2004) model.

The present model for crustal reverse-fault events predicts ground motions about 20-40% higher than those from crustal strike-slip and normal-fault events. This result is similar to those from many other models derived from overseas crustal events. The present model also indicates that interface events produce ground motions that are similar to those of crustal strike-slip events up to 0.4s but produce much smaller ground motions at longer periods. At 5.0s, the present model predicts 30% lower ground motions for interface events than for crustal strike-slip events. The present model predicts over 60% higher ground motions for slab events at a source distance of 40km than for crustal strike-slip events for periods up to 0.8s. At a 120km distance the spectral accelerations predicted for slab events are similar to those for the interface events. At periods beyond 0.8s, the spectral accelerations predicted for slab events decrease rapidly with increasing period. The difference between the factor for slab events and interface events is period- and source distance dependent, varying from a scale factor of 2.0 at a source distance of 40km for short and intermediate periods to a scale factor of 1.0 at all periods at a source distance of 120km (see that the source type factor for slab events at a source distance of 120km has nearly very close values to that of the interface event, Figure 5a), instead of a constant of 0.364 (a scale factor of 1.44) as in the Youngs *et al*. (1997) model.

In the present model, earthquake depth has a very large effect on the prediction of ground motions, especially at short periods. An earthquake at a depth of 80km may produce ground motions 2.5 times those of an earthquake of 15km deep, at the same source distance. The present model is valid for earthquakes with a depth up to 120km.

The most important feature of the present model is that site class terms, rather than individual site terms, are used to account for site effects. This method is consistent with the methodology that is most commonly used for developing attenuation models. This approach is believed to be capable of modelling source terms without causing source effects to be shifted into individual site terms. Using site class terms is likely to retain the statistical power of ground motion data from stations with few records.

In the present model, predictions for subduction events in the near-source region are largely constrained by shallow crustal events from the western part of the USA. Adding records from large subduction events within a distance of 50km could possibly result in improvement.

Our residual analyses on the present model shows that, at long periods, a magnitude-squared term is necessary for crustal and subduction earthquakes. However, the coefficient of the magnitude-squared term for subduction slab events is positive at short periods and negligible at long periods. Our analyses also show that a depth-dependent anelastic attenuation term would improve the fitting of the model for subduction for slab events, similar to the findings of Nishimura & Horike (2003) and

Eberhart-Phillips & McVerry (2004). Due to the limited time available for the present study these aspects were not fully investigated. Due to the lack of magnitude-squared term in the present model, spectra at long periods from very large crustal events are over-predicted. For example, the spectral accelerations for an M_w=7.8 crustal earthquake are over-estimated by factors of approximately 1.2, 1.3 and 1.5 at 1.0, 2.0 and 4.0s respectively, while the spectra at periods 0.5s or less are well predicted by the present model. These factors are approximately a linear function of $\log_e(T)$. This aspect needs to be considered if the present model is used to calculate long-period response spectra for very large crustal earthquakes.

Acknowledgements

The authors thank Drs. Tomotaka Iwata and Haruko Sekiguchi of DPRI, Kyoto University for their generous support. We also thank Dr. Jim Cousins for reviewing the manuscript and their constructive comments. The support from the Japanese Society for Promotion of Science for Dr. John X. Zhao during his fellowship leave in Kyoto University in 2000 is appreciated.

References

Abrahamson, N.A. and Youngs, R.R. (1992), A stable algorithm for regression analysis using the random effect model, *Bull. Seism. Soc. Am.*, **82**, 505-510.

Abrahamson, N.A. and Silva, W.J. (1997), Empirical response spectral attenuation relations for shallow crustal earthquakes, *Seism. Res. Lett.*, **68**, 94-127.

Building Seismic Safety Council (BSSC) (2000), The 2000 NEHRP Recommended Provisions for New Buildings and Other Structures, Part I (Provisions) and Part II (Commentary), FEMA 368/369, Washington DC.

Eberhart-Phillips, D. and McVerry, G. (2003) Estimating slab earthquakes response spectra from a 3D Q model, *Bull. Seism. Soc. Am*, **93**, 2649-2663.

Fukushima, Y. Irikura, K., Uetake T., and Matsumoto, H. (2000), Characteristics of observed peak amplitude for strong ground motion from the 1995 Hyogo-ken Nanbu (Kobe) earthquake, *Bull. Seism. Soc. Am*, **90**, 545-565.

Kobayashi, S., Takahashi, T., Matruzaki, S., Mori, M., Fukushima, Y., Zhao, J.X. and Somervill, P.G. (2000), A spectral attenuation model for Japan using digital strong motion records of JMA87 type, 12th *World Conf. Earthq. Eng*., Auckland, New Zealand.

Molas, G.L. and Yamazaki, F. (1995), Attenuation of earthquake ground motion in Japan including deep focus events, *Bull. Seism. Soc. Am*, **85**, 1343-1358.

Nishimura, T. and Horike, M. (2003), The attenuation relationships for peak ground accelerations for the horizontal and the vertical components inferred from the Kyoshin network data, *J. Structure Const. Eng., AIJ*, No. 571, 63-70 (in Japanese).

Si, H. and Midorikawa, S. (1999), New attenuation relationships for peak ground acceleration and velocity considering effects of fault type and site condition, *J. Structure Const. Eng., AIJ*. No. 523, 63-70 (in Japanese).

Takahashi, T., Saiki, T., Okada, H. Irikura, K., Zhao, J.X.,, Zhang, J., Thoi, H.K., Somerville, P.G., Fukushima, Y. and Fukushima, Y. Attenuation models for response spectra derived from Japanese strong-motion records accounting for tectonic source types *13th World Conf. Earthq. Eng.*, 2004 Vancouver, B.C., Canada, paper No. 1271.

Youngs, R.R., Chiou, S.-J., Silva, W.J. and Humphrey, J.R. (1997), Strong ground motion attenuation relationships for subduction zone earthquakes, *Seism. Res. Lett.*, **68**, 94-127.

Zhao, J.X., Irikura, K., Zhang, J., Fukushima, Y., Somerville, P.G., Saiki, T., Okada, H. and Takahashi, T. (2004) Site classification for strong-motion stations in Japan using h/v response spectral ratio, *13th World Conf. Earthq. Eng.*, Vancouver, B.C., Canada, paper No. 1278.

Figure 1 **Magnitude-distance distribution for (a) data from Japan; (b) overseas data; (c) magnitude-focal depth distribution; and (d) source distance-focal depth distribution of Japanese data.**

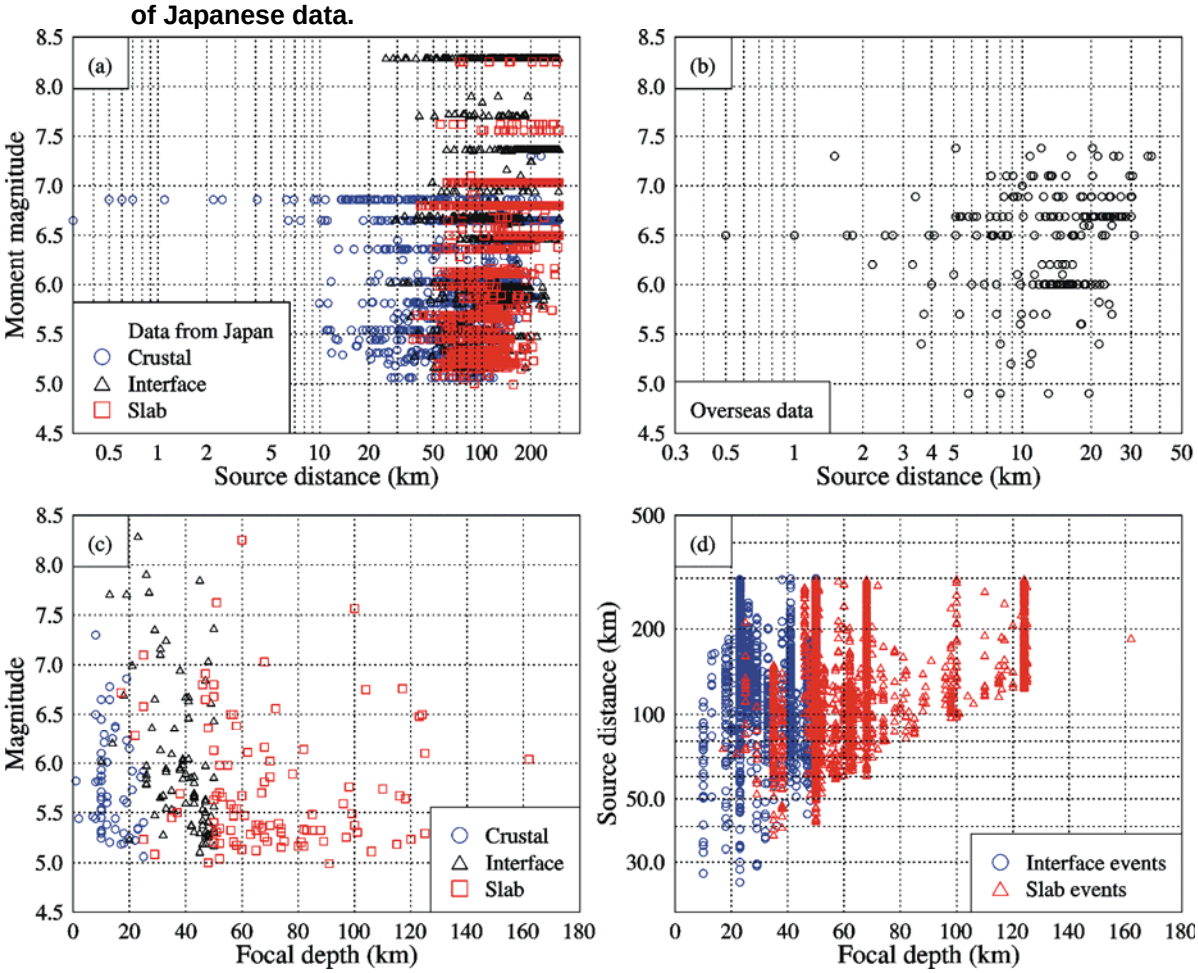

Figure 2 **Comparison predicted PGA by the present model with the PGAs from earthquakes with magnitude 6.0 or larger, (a) for crustal and interface events and (b) for slab events. The PGAs have been normalized to M_W = 7.0 at a focal depth of 30 km for SC II site conditions.**

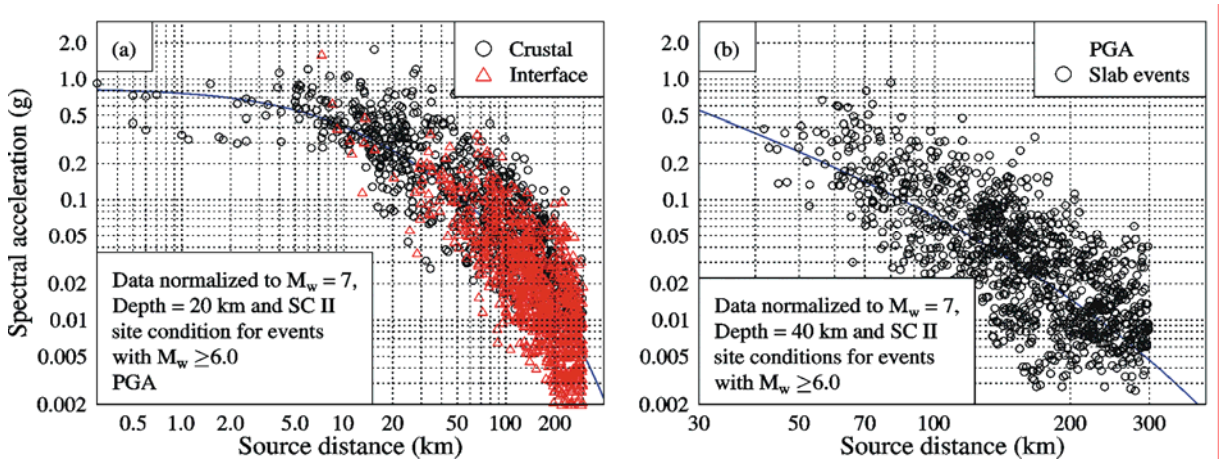

Figure 3 Comparison of predicted PGA by the present model with those of (a) Fukushima *et al*. (2000) and Si & Midorikawa (1999) for crustal strike-slip events and (b) Si & Midorikawa for slab events, with the mean site terms for magnitudes 5, 6, 7 and 8.

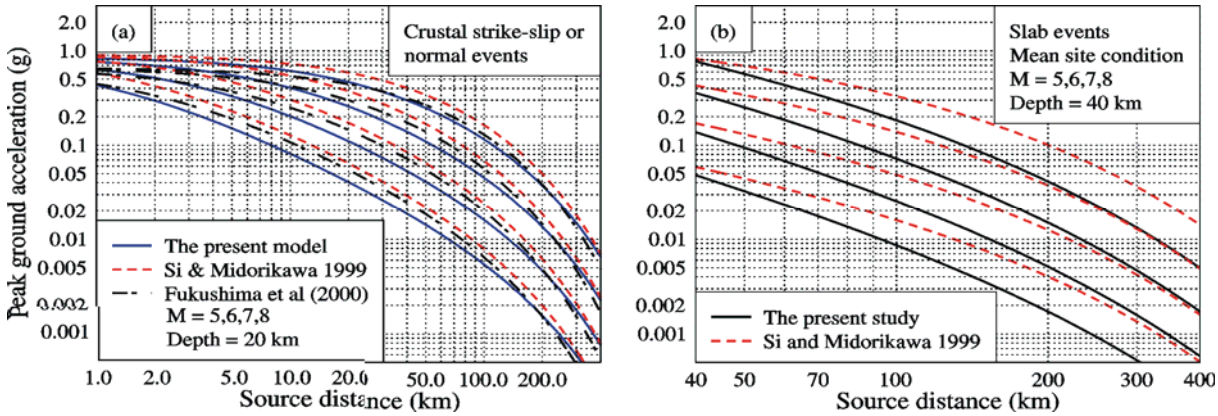

Figure 4 Scale factors for (a) source types and reverse crustal events with respect to strike-slip & normal crustal events; and for (b) focal depth with respect to events of focal depth h=15 km or less. Note that scale factors for slab events are shown for 40, 60, 80 and 120km source distances in (a).

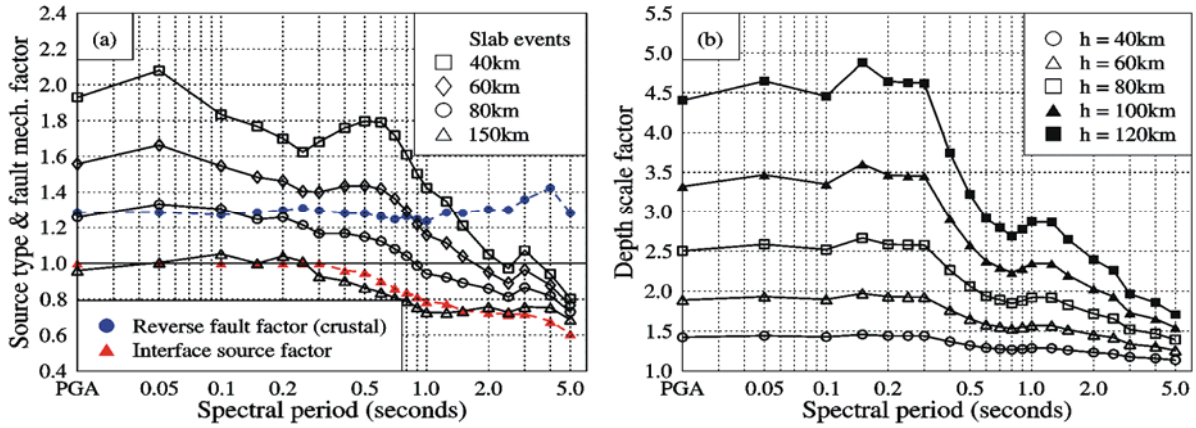

Figure 5 Total standard deviation, (a) crustal events; and (b) subduction events.

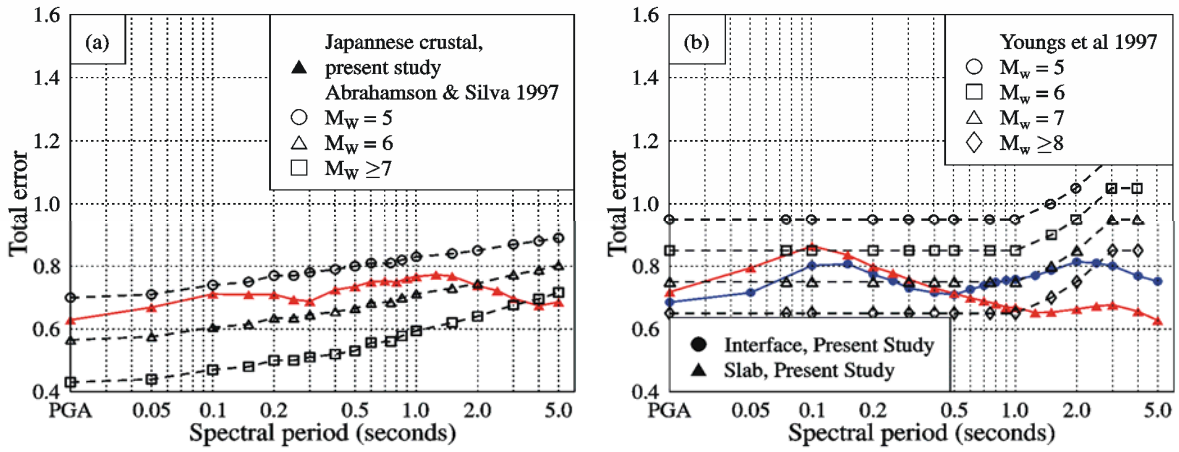

Figure 6 Illustration of site effects, (a) site amplification factors with respect to SC I sites; and (b) spectral shape for crustal strike-slip and normal events for all four site classes.

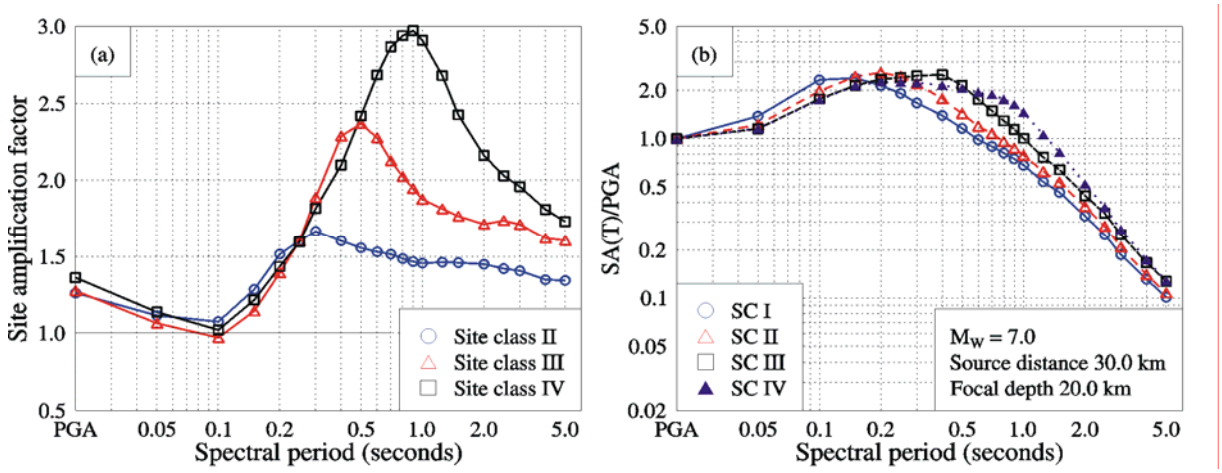

Figure 7 Pseudo-velocity spectra calculated for crustal strike-slip and normal events, interface events and slab events with a magnitude of 7.0 and a depth of 20km for SC II sites at a source distance of (a) 40km and (b) 60km; the spectra from a slab event at a depth of 40km are also presented for comparison.